TESLA cavity modeling and digital implementation in FPGA technology for control system development

Tomasz Czarski, Krzysztof T.Pozniak, Ryszard S.Romaniuk,
Warsaw University of Technology, Poland
Stefan Simrock
DESY, Hamburg, Germany

Abstract

The electromechanical model of the TESLA cavity has been implemented in FPGA technology for real-time testing of the control system. The model includes Lorentz force detuning and beam loading effects. Step operation and vector stimulus operation modes are applied for the evaluation of a FPGA cavity simulator operated by a digital controller. The performance of the cavity hardware model is verified by comparing with a software model of the cavity implemented in the MATLAB system. The numerical aspects are considered for an optimal DSP calculation. Some experimental results are presented for different cavity operational conditions.

PACS: 07.05.Dz, 07.50.-e, 29.17.+w, 29.50.+v

Keywords: superconducting cavity control, TESLA accelerator, X-ray FEL, LLRF – Low Level Radio Frequency, control theory, FPGA, DSP, VHDL, system simulation, cavity controller, cavity simulator.

Corresponding author: R.S.Romaniuk, Institute of Electronic Systems, WUT
Nowowiejska 15/19, 00-665 Warsaw, Poland, rrom@ise.pw.edu.pl

Paper published in NIMA, Vol. 556, Issue 2, 15 January 2006, pages 565-576

1. Introduction

The majority of existing accelerators are controlled by analog control systems. A fully digital solution of such systems has recently become possible with the advent of FPGA chips equipped with DSP capabilities. A new generation of digital controllers may integrate new tasks like: system identification and simulation, continuous and multichannel measurements, massive data acquisition, continuous diagnostics and exception handling, introduction of real-time feedback between the beam quality (electrical and optical) and system parameters, building a rich database of the system behavior in changing working conditions, etc. The above tasks rest on the assumption that the idle time, of the accelerator working in pulsed mode, may be efficiently used for the intensive DSP calculations. The introduction of new features is expected to result in: increased system safety, shorter design time, less human resource requirements, less consumed material and occupied space by the control-diagnostic system, less power consumption, increased reliability in adverse environments and lower cost.

The TESLA accelerator uses nine-cell superconducting niobium resonators to accelerate electrons and positrons. The acceleration structure is operated in a standing π-mode wave at the frequency of 1,3 GHz. The RF oscillating field is synchronized with the motion of a particle moving at the velocity of light across the cavity (see figure 1). The LLRF (low level radio frequency) cavity control system for the TESLA project has been developed in order to stabilize the accelerating fields of the resonators. The control section, powered by one klystron, may consist of many cavities. One klystron supplies the RF power of 10 MW to the cavities through the coupled waveguide with a circulator. The cavities are driven with pulses of 1.3 ms in duration and the average accelerating gradients of 25 MV/m. The control feedback system regulates the vector sum of the pulsed accelerating fields in multiple cavities. The fast amplitude and phase control of the cavity field is accomplished by modulation of the signal driving the klystron. The cavity RF signal is down-converted to an intermediate frequency of 250 kHz preserving the amplitude and phase information. The ADC and DAC converters link the analog and digital parts of the system. The digital signal processing is applied for the detection of the field vector as the complex envelope represented by real - I (in-phase) and imaginary – Q (quadrature) components (I/Q detector). The digital controller stabilizes the complex envelope of the cavity wave, according to the desired set point. Additionally, the adaptive feed-forward is applied to improve the compensation of repetitive perturbations induced by the beam loading and by the dynamic Lorentz force detuning.

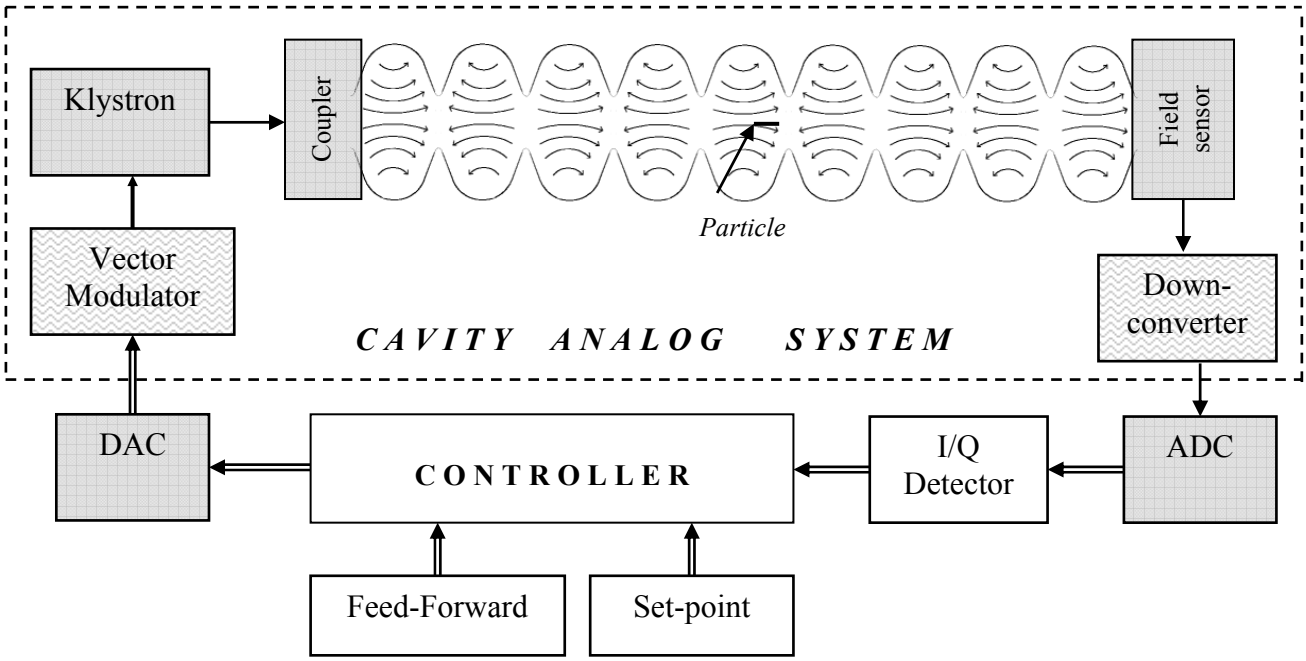

Figure 1. Cavity environment and simplified block diagram of the cavity control system

The theoretical verification of the existing superconducting cavity model [1-3] lead to the synthesis of a digital algorithm efficiently implemented in the FPGA structure. This cavity simulator was used for evaluation of the control algorithms and for investigation of the optimal control method. The FPGA hardware implementation of the cavity model is intended for real time operation.

2. The cavity model

2.1 Electrical circuit model

The following considerations are limited to a single cavity represented as LCR circuit coupled to a waveguide driven by a klystron. This approach is sufficient for the purpose of cavity control modeling [1-3]. The circuit model of the cavity environment is presented in figure 2. The currents (J) and voltages (U) are represented in *Laplace space*. The klystron as a power amplifier is modeled by the RF current generator J_k driving the waveguide via a circulator. The waveguide, as a transmission line, is parameterized by characteristic impedance Z_0 and time delay T_w. The cavity is represented as resonant LCR circuit with impedance $Z_c(\mathbf{s}) = (1/R + \mathbf{s}C + 1/\mathbf{s}L)^{-1}$ coupled to the waveguide. Beam loading is modeled as a current source $-J_b$ supplied by the electromagnetic field of the cavity. The bunched beam current has ~2 ps pulse duration, 1 MHz rate and an average value of 8 mA.

The *forward wave* is represented by current J_f and voltage $U_f = J_f \cdot Z_0$. The *reflected wave*, represented by current J_r and voltage $U_r = J_r \cdot Z_0$ is terminated by the circulator load, matched to the waveguide ($J_f = J_k$). Superposition of the *forward* and *reflected wave*, represented by current $J_1 = J_f - J_r$ and voltage $U_1 = U_f + U_r = (2J_k - J_1)\cdot Z_0$ drives the coupler, which converts the signals according to transformation ratio 1:N. The output signals of the coupler are represented by current $J_2 = J_1/N$ and voltage $U_2 = NU_1 = U_c = (2J_k/N - J_1/N)\cdot N^2 Z_0$. Superposition of the output current of the coupler and beam loading results in the cavity current J_c and cavity voltage U_c, related by impedance Z_c.

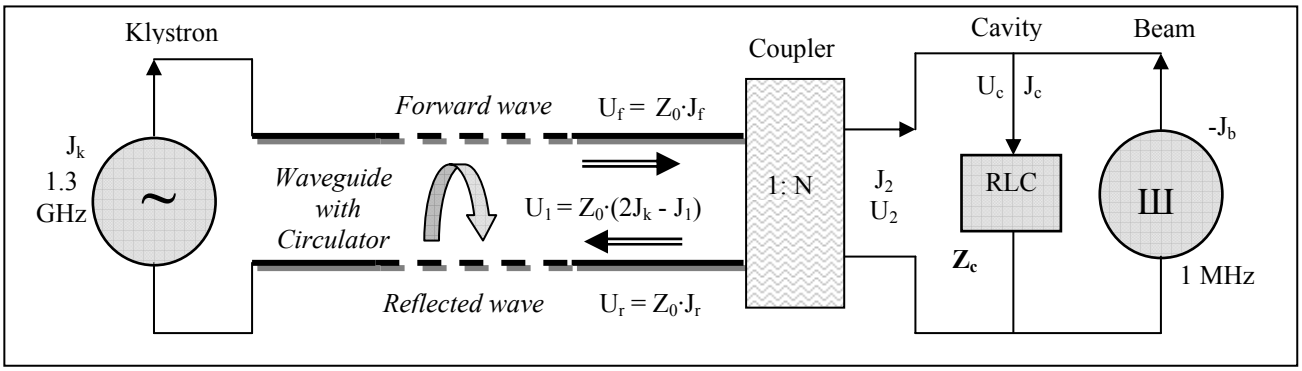

Figure 2. Circuit model of cavity environment

Introducing the cavity loaded impedance $Z_L = N^2 Z_0 \| Z_c$ (parallel connection) and defining the transformed generator current $J_g \equiv J_k / N$, results in the cavity voltage $U_c = (2J_g - J_b)\cdot Z_L = J \cdot Z_L$. Therefore, the cavity loaded impedance $Z_L(\mathbf{s})$ can be represented by the transfer function in the corresponding forms:

$$Z_L(\mathbf{s}) = (1/R_L + \mathbf{s}C + 1/\mathbf{s}L)^{-1} = \omega_0 \cdot \rho \mathbf{s} / (\mathbf{s}\omega_0/Q_L + \mathbf{s}^2 + \omega_0^2) = \omega_{1/2} \cdot R_L / (\omega_{1/2} + (\mathbf{s}^2 + \omega_0^2)/2\mathbf{s}) \qquad (1)$$

where, the following *secondary* parameters (derived from the *primary* LRC parameters) are applied: resonance frequency $\omega_0 = 2\pi f_0 = (LC)^{-½}$, characteristic resistance $\rho = (L/C)^{½}$, shunt resistance $R_L \equiv R \| N^2 \cdot Z_0$, loaded quality factor $Q_L = R_L/\rho$, half-bandwidth (HWHM)
$\omega_{1/2} = 2\pi f_{1/2} = 1/2CR_L = \omega_0/2Q_L$.

Due to the stability of the RF generator frequency ω_g, and narrow resonator bandwidth, the cavity voltage can be modeled in the *time domain* as *analytical signal* represented as a vector or phasor in the complex domain:

$$\mathbf{u}(t) \equiv [u_r, u_i] \equiv u_r + \boldsymbol{i}u_i = a(t)\cdot(\cos(\omega_g t + \varphi(t)) + \boldsymbol{i}\cdot\sin(\omega_g t + \varphi(t))) = a(t)\cdot\exp(\boldsymbol{i}\cdot(\omega_g t + \varphi(t))), \qquad (2)$$

where u_r is a real signal and u_i its *Hilbert transform*; amplitude $a(t)$ and phase $\varphi(t)$ are slowly time-varying parameters relative to the period of the RF signal carrier.

The cavity current is modeled as an *analytical signal* $\mathbf{j}(t) = 2\mathbf{j}_g(t) - \mathbf{j}_b(t)$, where $\mathbf{j}_b$ corresponds to the ω_g Fourier component of the beam loading current. The relation between the current and the voltage is given in *Laplace space*:

$$\mathbf{U}(\mathbf{s}) = \mathbf{J}(\mathbf{s})\cdot Z_L(\mathbf{s}) \tag{3}$$

where $\mathbf{U}(\mathbf{s})$ and $\mathbf{J}(\mathbf{s}) = 2\mathbf{J}_g(\mathbf{s}) - \mathbf{J}_b(\mathbf{s})$, are Laplace transforms of the *analytical signal* for the voltage and current respectively.

The low level RF representation of the cavity signal in the *time domain* is the *complex envelope* derived from the complex demodulation (down conversion) of the *analytical signal,* which is obtained by applying the operator $\exp(-\boldsymbol{i}\omega_g t)$ for a given frequency ω_g. *Vice versa*, the complex modulation (up conversion) of the *envelope* is obtained by applying the operator $\exp(\boldsymbol{i}\omega_g t)$ and yields the *analytical signal* for a given frequency ω_g. The *complex envelope* for the cavity current $\mathbf{i}(t)$ and voltage $\mathbf{v}(t)$ can be represented as a vector or phasor by its real I - in-phase, and imaginary Q - quadrature components as follows (for the voltage case):

$$[I, Q]_{voltage} \equiv \mathbf{v}(t) \equiv [v_r, v_i] \equiv v_r + \boldsymbol{i}v_i \equiv \mathbf{u}(t)\cdot\exp(-\boldsymbol{i}\omega_g t) = a(t)e^{\boldsymbol{i}\varphi(t)} \equiv [a(t)\cos\varphi(t), a(t)\sin\varphi(t)]. \tag{4}$$

The signal relation is modeled by the flow graph according to figure 3.

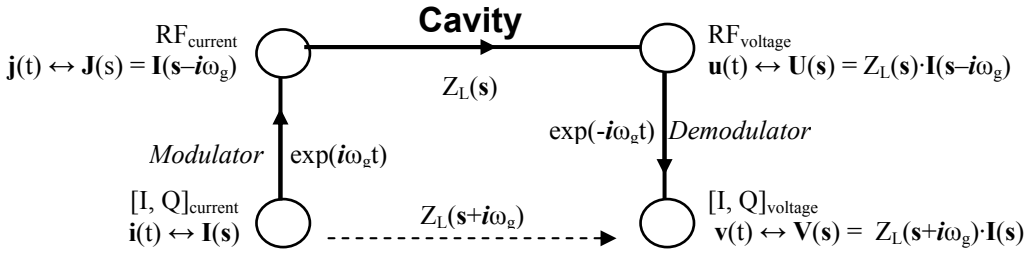

Figure 3. Cavity signal-flow graph for *complex envelope* and *analytical signal* (left-right arrow ↔ means *Laplace transformation*)

The successive operations, presented by the signal-flow graph in figure 3, yield the direct relation between the cavity input and output

$$\mathbf{V}(\mathbf{s}) = \mathbf{I}(\mathbf{s})\cdot Z_L(\mathbf{s}+\boldsymbol{i}\omega_g), \tag{5}$$

where $\mathbf{V}(\mathbf{s})$ and $\mathbf{I}(\mathbf{s}) = 2\mathbf{I}_g(\mathbf{s}) - \mathbf{I}_b(\mathbf{s})$, are the Laplace transforms of the *complex envelope* for the voltage and the current respectively.

The resultant cavity transfer function is transformed to a low-pass filter. The analytical form of impedance can be simplified for signals with narrow spectral range in comparison with the generator frequency close to the cavity resonance frequency. Then, for $|\mathbf{s}| << \omega_g \approx \omega_0$ yields: $Z_L(\mathbf{s}+\boldsymbol{i}\omega_g) \approx \omega_{1/2}\cdot R_L/(\mathbf{s} + \omega_{1/2} - \boldsymbol{i}\Delta\omega)$, where the cavity detuning is $2\pi\Delta f = \Delta\omega \equiv \omega_0 - \omega_g$.

The *complex envelope* relation for the cavity signals is written in *Laplace space* as follows:

$$\mathbf{s}\cdot\mathbf{V}(\mathbf{s}) = (-\omega_{1/2} + \boldsymbol{i}\Delta\omega)\cdot\mathbf{V}(\mathbf{s}) + \omega_{1/2}\cdot R_L\cdot\mathbf{I}(\mathbf{s}). \quad (6)$$

Moving to the *time domain* yields the *state space* equation with $\mathbf{v}(t)$ as a state vector of the cavity electrical model:

$$d\mathbf{v}(t)/dt = \mathbf{A}_e\cdot\mathbf{v}(t) + \omega_{1/2}\cdot R_L\cdot\mathbf{i}(t), \quad (7)$$

where $\mathbf{v}(t)$ and $\mathbf{i}(t) = 2\mathbf{i}_g(t) - \mathbf{i}_b(t)$ are the time dependent *complex envelopes* of the voltage and current respectively and $\mathbf{A}_e = -\omega_{1/2}+\boldsymbol{i}\Delta\omega$ is the phasor.

The resultant *state space* equation for the *complex envelope* depends only on the cavity bandwidth and detuning. This simple relationship for the cavity *envelope* allows for a control system modeling within the low-level frequency range. The phasor solution of the state-space equation for the current step input $\mathbf{i}_0$ is as follows

$$\mathbf{v}(t) = \mathbf{i}_0\cdot\omega_{1/2}\cdot R_L\cdot(\exp(\mathbf{A}_e\cdot t) - 1)/\mathbf{A}_e \text{ for time } t \geq 0. \quad (8)$$

The step response of the cavity voltage [I,Q] components and the corresponding envelope graph are presented in figure 4 for a driving current of i_0 = 32 mA (i_g=16 mA, i_b=0, R_L = 1560 MΩ, $f_{1/2}$ = 216 Hz, detuning range Δf = -400 ÷ +400 Hz).

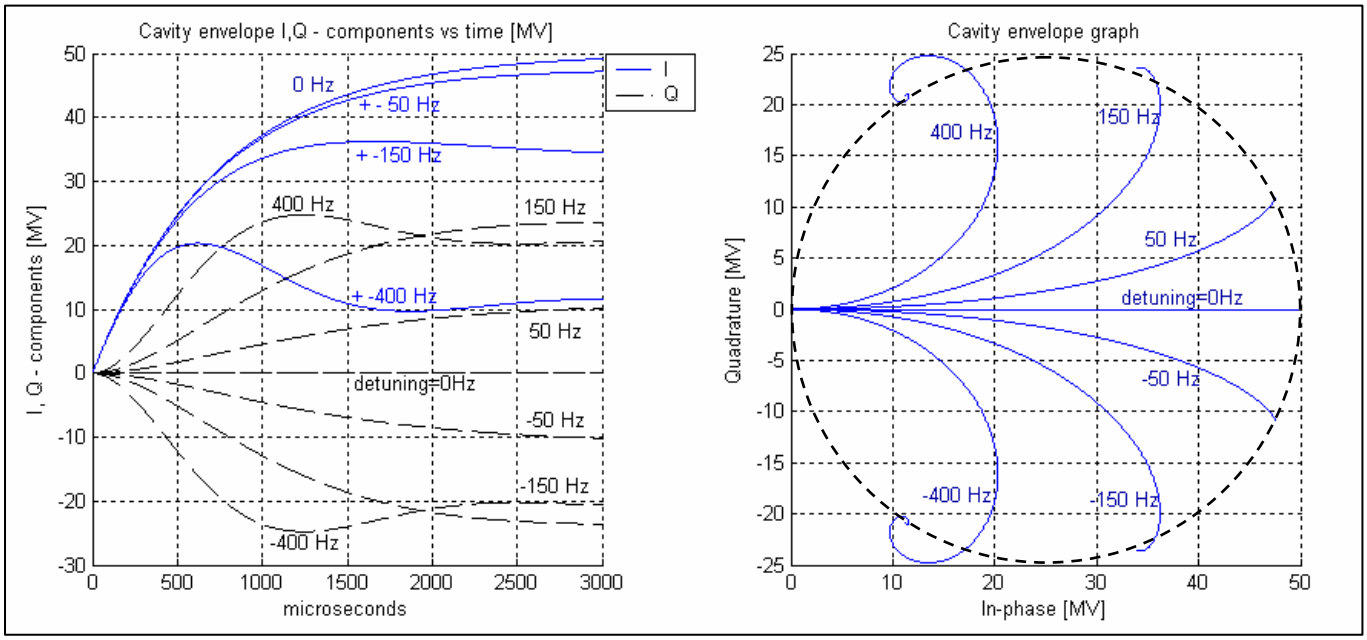

Figure 4. The step response of the cavity voltage envelope represented by [I,Q] – components and the corresponding envelope graph – trajectory of the [I, Q] vector for different detuning.

2.2. Electromechanical model

The cavity has a high loaded quality factor $Q_L \sim 3 \cdot 10^6$ and a narrow bandwidth of about 430 Hz (FWHM). The cavity is sensitive to mechanical distortion caused by microphonics and Lorentz force, changing the resonator frequency. The cavity model is non-stationary with a time varying *detuning* $\Delta\omega$. A value of the cavity detuning can be comparable to the cavity bandwidth in the real operation condition. This cavity parameter has two dominant deterministic components: the Lorentz force detuning and the initial *predetuning*. The mechanically biased *predetuning* attempts to compensate the EM forced detuning factor, during operation of the cavity. The mechanical model of the cavity describes the dynamic Lorentz force detuning which depends on the time varying field gradient [2]. It is based on a linear relationship for each of the independent mechanical modes of the cavity with resonance frequency f_m and mechanical quality factor Q_m for a given mode. Each of the mechanical

equation for the m-th mode:

$$d\mathbf{w}_m(t)/dt = \mathbf{A}_m \cdot \mathbf{w}_m(t) + \mathbf{B}_m \cdot v^2(t), \tag{9}$$

where $\mathbf{w}_m(t) = [\Delta\omega_m(t);\ d[\Delta\omega_m(t)]/dt]$ is the state vector and consists of the time-varying detuning $\Delta\omega_m(t)$ and its time derivative; $\mathbf{A}_{m[2x2]} = [\ 0,1;\ -(2\pi f_m)^2,\ -2\pi f_m/Q_m]$ is the system matrix; vector $\mathbf{B}_{m[2x1]} = [0;\ -\ (2\pi f_m)^2 \cdot K_m]$ is the input matrix where the parameter K_m is the Lorentz force detuning constant.

The resulting cavity detuning is $\Delta\omega(t) = \sum\Delta\omega_m(t) + \Delta\omega_0$, where $\Delta\omega_0$ is the initial *predetuning*.

The main parameters of the cavity electromechanical model are gathered in table 1. The three dominating modes are considered for the mechanical model.

The pure mechanical model is weakly damped. The dominating oscillations are caused by the mechanical modes (table 1) driven by the square of the field gradient.

Table 1.

CAVITY ELECTRICAL parameters	CAVITY MECHANICAL modes parameters
$f_0 = 1300$ ……resonance frequency [MHz] $\rho = 520$ ……..characteristic resistance [Ω] $Q_L = 3 \cdot 10^6$……..loaded quality factor $R_L = Q_L \cdot \rho = 1560$……..load resistance [MΩ] $f_{1/2} = f_0/2Q_L = 216$…….half band-width [Hz] $\Delta f = 390$ …….pre-detuning [Hz]	**f** = [235,290,450]……resonance frequencies vector [Hz] **Q** = [100,100,100]…… quality factor vector **K** = [0.4, 0.3, 0.2]……Lorentz force detuning constants vector [Hz/(MV)^2]

3. Digital processing of the cavity model

3.1 Discrete cavity model

A discrete processing of the cavity algorithm has been developed for a digital implementation of the cavity model. The continuous model of the cavity behavior, presented in equations (7) and (9), can be approximated by recursive calculations in a finite number of steps. Applying the Euler approximation for time the derivative of a general variable x: $d\mathbf{x}/dt \approx (x_{n+1} - x_n)/T$, yields for successive n-th and (n+1)-th samples, with time interval T and with identity matrix **1,** the following recursive equations, respectively:

- for the electrical model (7) in the vector representation with matrix $\mathbf{A}_e = [-\omega_{1/2}, -\Delta\omega; \Delta\omega, -\omega_{1/2}]$,

$$\mathbf{v}_{n+1} = (\mathbf{1} + T\cdot\mathbf{A}_e)\cdot\mathbf{v}_n + T\cdot\omega_{1/2}\cdot R_L\cdot\mathbf{i}_n, \text{ where } \mathbf{i}_n = 2(\mathbf{i}_g)_n - (\mathbf{i}_b)_n, \tag{10}$$

- for the mechanical m-th mode (9),

$$(\mathbf{w}_m)_{n+1} = (\mathbf{1} + T\cdot\mathbf{A}_m)\cdot(\mathbf{w}_m)_n + T\cdot\mathbf{B}_m\cdot(v^2)_n. \tag{11}$$

Applying simplified notation by ignoring time indices and by introducing new symbols yields, respectively,

- for the electrical model:

$$\mathbf{v} = \mathbf{E}*\mathbf{v} + \mathbf{ig} - \mathbf{ib}, \tag{12}$$

where $\mathbf{E} = [1-T\cdot\omega_{1/2}, -T\cdot\Delta\omega; T\cdot\Delta\omega, 1-T\cdot\omega_{1/2}]$ is the discrete system matrix and $\mathbf{ig} = T\cdot\omega_{1/2}\cdot R_L\cdot 2\mathbf{i}_g$ is the unified input signal for the generator and $\mathbf{ib} = T\cdot\omega_{1/2}\cdot R_L\cdot\mathbf{i}_b$, for the beam loading,

- for the m-th mechanical mode:

$$\mathbf{w}_m = (\mathbf{1}+T\cdot\mathbf{A}_m)\cdot\mathbf{w}_m + T\cdot\mathbf{B}_m\cdot v^2. \tag{13}$$

Applying the common state vector **w** (dim = 6 x 1) and the common matrix **A** (dim = 6 x 6) and the common vector **B** (dim = 6 x 1)**,** for the mechanical model with 3 modes, yields:

$$\mathbf{w} = \mathbf{A}*\mathbf{w} + \mathbf{B}*v^2, \tag{14}$$

where the partial vector and matrices with indices range (2m-1: 2m) for the m-th mode are defined as: $\mathbf{w}(2m\text{-}1{:}2m) = \mathbf{w}_m$, $\mathbf{A}(2m\text{-}1{:}2m, 2m\text{-}1{:}2m) = \mathbf{1}_2+T\cdot\mathbf{A}_m$, $\mathbf{B}(2m\text{-}1{:}2m) = T\cdot\mathbf{B}_m$ for m = 1:3.

The resultant detuning of the cavity is $\Delta\omega = \sum\mathbf{w}(2m\text{-}1) + w0$, where w0 is the initial *predetuning*.

The discrete cavity algorithm, for the electrical and mechanical parallel iterative processing, has been implemented by applying Matlab code with the sampling time T= 1μs.

3.2 Cavity simulator algorithm

The functional diagram of the cavity digital simulator algorithm, according to the electromechanical model, is presented in figure 5. The electrical part of the cavity simulator is implemented in an arithmetical function block using DSP functions. The arithmetic procedure is realized according to the *state space* relation with state vector **v** representing [I, Q] components of the cavity output *envelope*. The discrete *system matrix* **E** depends on the cavity detuning $\Delta\omega$ and the cavity bandwidth $\omega_{1/2}$. A normalized current generator with input signal **ig** and the beam **ib**, drives the DSP unit. The non-stationary detuning $\Delta\omega$ is a parameter of the matrix **E**. The input and output registers correspond to the time delay of cavity environment (waveguide). The intermediate frequency IF modulator converts the cavity output vector to the signal v_m of frequency 250 kHz (reciprocal operation to the I/Q detection).

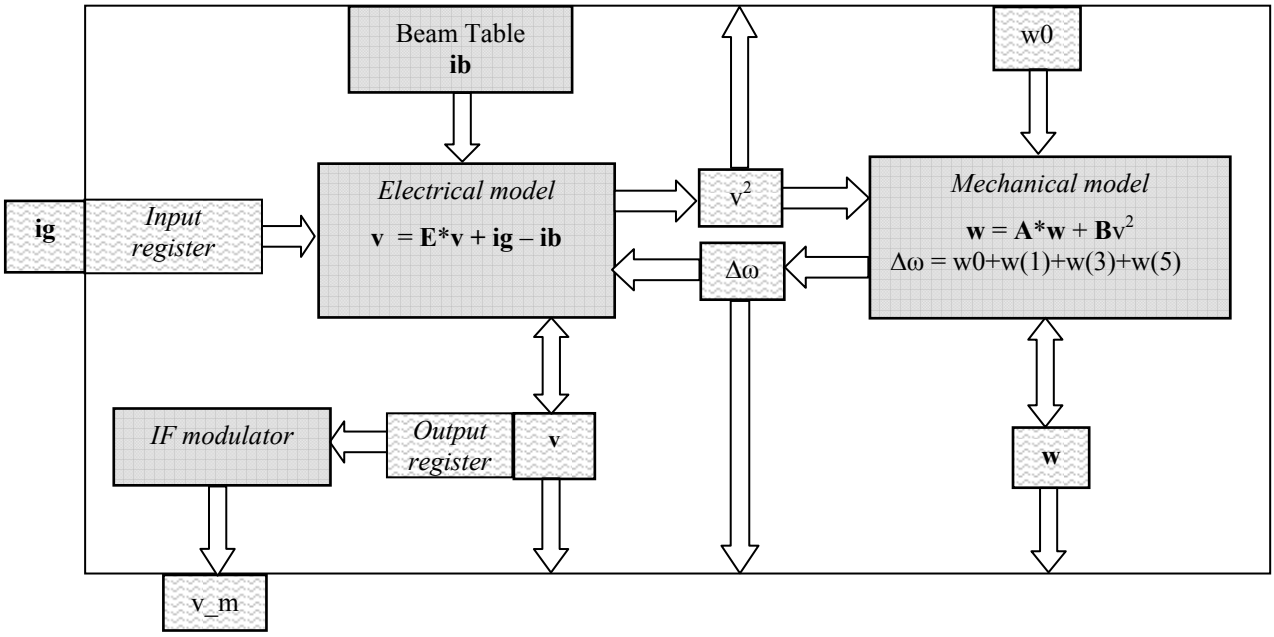

Figure 5. Functional diagram of the cavity simulator algorithm

The mechanical model of the cavity is implemented in the DSP unit, according to the *state space* relation, with the state vector **w**. The time-varying detuning and its time derivative are two state-variables for each mechanical mode. The system matrix **A** and the vector **B** depend on the following cavity parameters: the resonance frequency, the quality factor and the Lorentz force-detuning constant for each mechanical mode. Each of the mechanical modes is driven by the square of the cavity field gradient v^2 generated from the electrical part of the

model. Three dominating resonance frequencies according to the table 1 are considered in the cavity model and the superposition of all modes, together with the initial *predetuning* w0, yield the resultant detuning $\Delta\omega$.

3.3 Cavity controller algorithm

A model of the control system has been developed to investigate different operational conditions of the cavity. The functional diagram of digital controller algorithm is presented in figure 6. The input signal v_m of intermediate frequency f_i= 250 kHz from the cavity simulator is demodulated by the I/Q detector unit. The external [I, Q] vector can be selected by the MUX switch. The resultant cavity voltage *envelope* [I, Q] is calibrated, so as to compensate the channel attenuation and phase shifting of individual cavities. The Set-Point table contains a signal level, which is compared to the actual cavity voltage. The multiplier, working as a proportional controller, amplifies the error signal according to the data from the GAIN table and closes the feedback loop. The Feed-Forward table is applied and the resultant output signal **ig** can drive the cavity simulator.

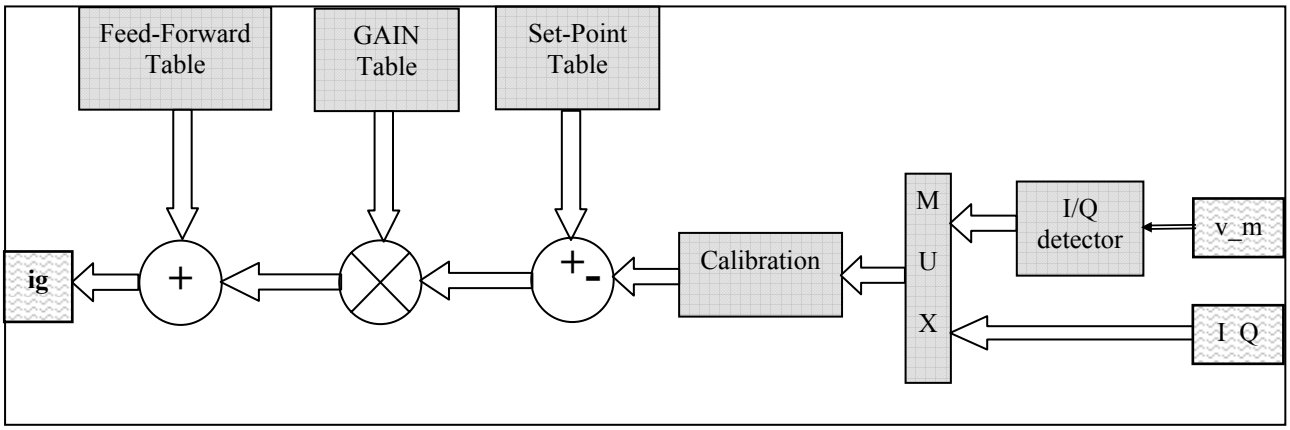

Figure 6. Functional diagram of the controller algorithm

3.4. DSP modeling and numerical optimization

The hardware implementation of the cavity model (discrete one) requires numerical care due to the limited resolution of the parameters and variables of the DSP. Normalization and scaling of the parameters and variables is an essential preparation for the DSP implementation with fixed point arithmetic. The actual range of the involved values extends up to seven decades (~2^{23}) for the cavity model. The best numerical accuracy for each linear operation can be achieved by preceding scaling (multiplication by power of two) and matching the values within the given N-bit resolution range, common for all involved quantities. The

range of the scaled parameters and the maximum values of the variables has been stretched to $\pm 2^{N-1}$ for each operation. Concluding the DSP operation, the obtained product is rescaled by bit shifting (division by power of two) to preserve its original normalization.

The main arithmetic processing, for each actual variable x_i, is a linear combination of the corresponding variables x_k with the parameter a_{ik} as follows: $x_i = \sum_k a_{ik} x_k$. The equivalent DSP operation is: $X_i = \sum_k A_{ik} X_k / S_{ik}$, with the scaled variable $X_i = s_i \cdot x_i$ with a scaling factor s_i, the scaled parameter $A_{ik} = s_{ik} \cdot a_{ik}$ with a scaling factor s_{ik}, the scaled variable $X_k = s_k \cdot x_k$ with scaling factor s_k, and the resultant rescaling factor $S_{ik} = s_{ik} \cdot s_k / s_i$. The number of bits equals to $\log_2(S_{ik})$ for the rescaling shift and for each multiplication.

The discrete cavity model from par.3.1., was adapted for the hardware implementation. The scaled model with integer-valued N-bit resolution was developed in the Matlab system as the pattern for the VHDL coding for the FPGA implementation. The numerical accuracy of the digital model was tested for different bit resolutions, and diverse scaling factors. The full bit resolution of the MATLAB cavity model, with normalized parameters and variables, was considered as a reference.

The relative step response is shown in fig.7 for all variables for the 18-bit resolution model compared to the reference with full resolution. Two cavity models (digital 18-bit resolution and full resolution one) were driven with the same input signal generator, equivalent to ~14,7 mA current pulse. The total time of the simulation is 10000 μs and is long compared to the real operating pulse of 1500 μs. Due to the good agreement the curves for two models are hardly distinguishable.

The relative mean square error of the complex envelope Err(N) for N-bit resolution was calculated for n steps according to the expression:

$$Err(N) = \sum |(\mathbf{V}_N)_k - (\mathbf{V}_{ref})_k|^2 / \sum |(\mathbf{V}_{ref})_k|^2, \quad \text{for } k = 1{:}n, \tag{15}$$

where $(\mathbf{V}_{ref})_k$ is the complex sample of the reference envelope for the k-th step, $(\mathbf{V}_N)_k$ is the complex sample of the N-bit resolution envelope for the k-th step.

The 18-bit resolution cavity model was considered for the final hardware realization with the relative mean square error Err(18) = 5.1e-3. The results for different bit resolutions are presented in fig.8. However, for nonlinear systems like this they depend on the detailed simulation conditions.

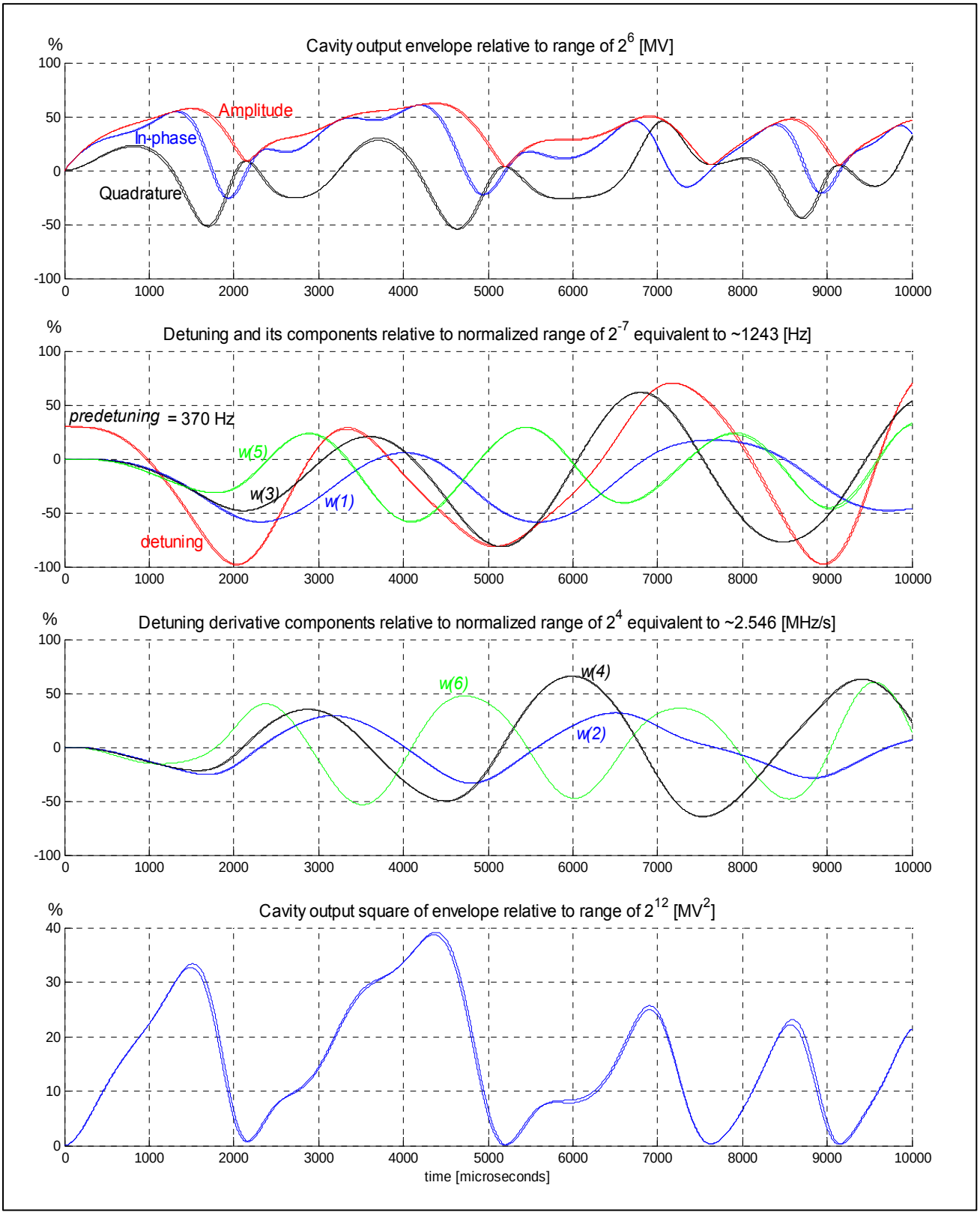

Figure 7. Relative step response for the 18-bit resolution model compared to the reference with full resolution (curves are hardly distinguished for two models).

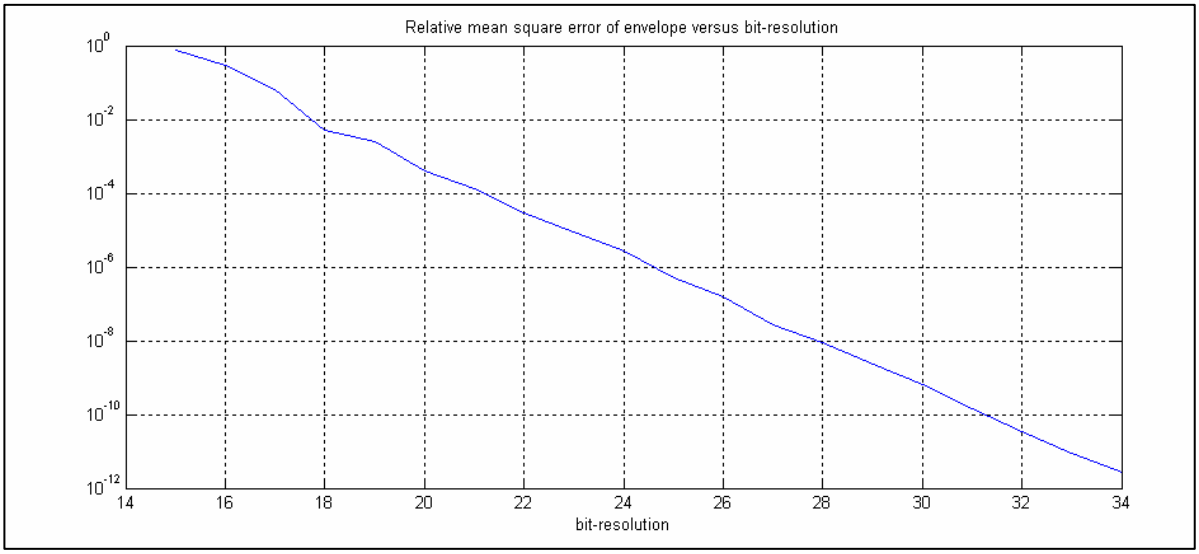

Figure 8. Relative mean square error of complex envelope for different bit-resolution of cavity model (total time of the simulation - 10000 μs).

The 18-bit resolution version of the FPGA cavity simulator is expected to be quite sufficient for this simulation. The limited validity of the heuristic mechanical model of the cavity and 14-bit resolution of the preferred analog-to-digital converter do not require a resolution of better quality. The main parameters of the FPGA simulator are combined in table 2.

Table 2

DSP resolution	DAC and ADC Resolution	Sampling time	Minimum Processing time	Maximum carrier frequency
18 [bit]	14 [bit]	1 μs	200 [ns]	1.25 [MHz]

4. FPGA based cavity simulator integrated with controller

A hardware layer of the cavity simulator and controller system (SIMCON) is realized with the commercial development kit [4]. The kit consists of the main board (MB) integrated with a daughter board (DB). The DB is realizing the hardware DSP algorithms. The DB possesses two fast 14-bit, 65MHz ADC and DAC and a FPGA VirtexII chip equipped with 18x18 bit multiplication circuits. The adaptation of the kit to the needs of the user standard is realized by embedding it on a carrier board 6HE EURO, as presented in fig.9. The SIMCON card occupies two slots in the VME 6U crate. The power supply is provided either from the VME bus or from the power unit provided with the board. The Enhanced Parallel Port (EPP)

protocol is used to communicate with the board because the EPP has a simple implementation in the FPGA chip. The hardware realization of the interface was described in detail in [5-7].

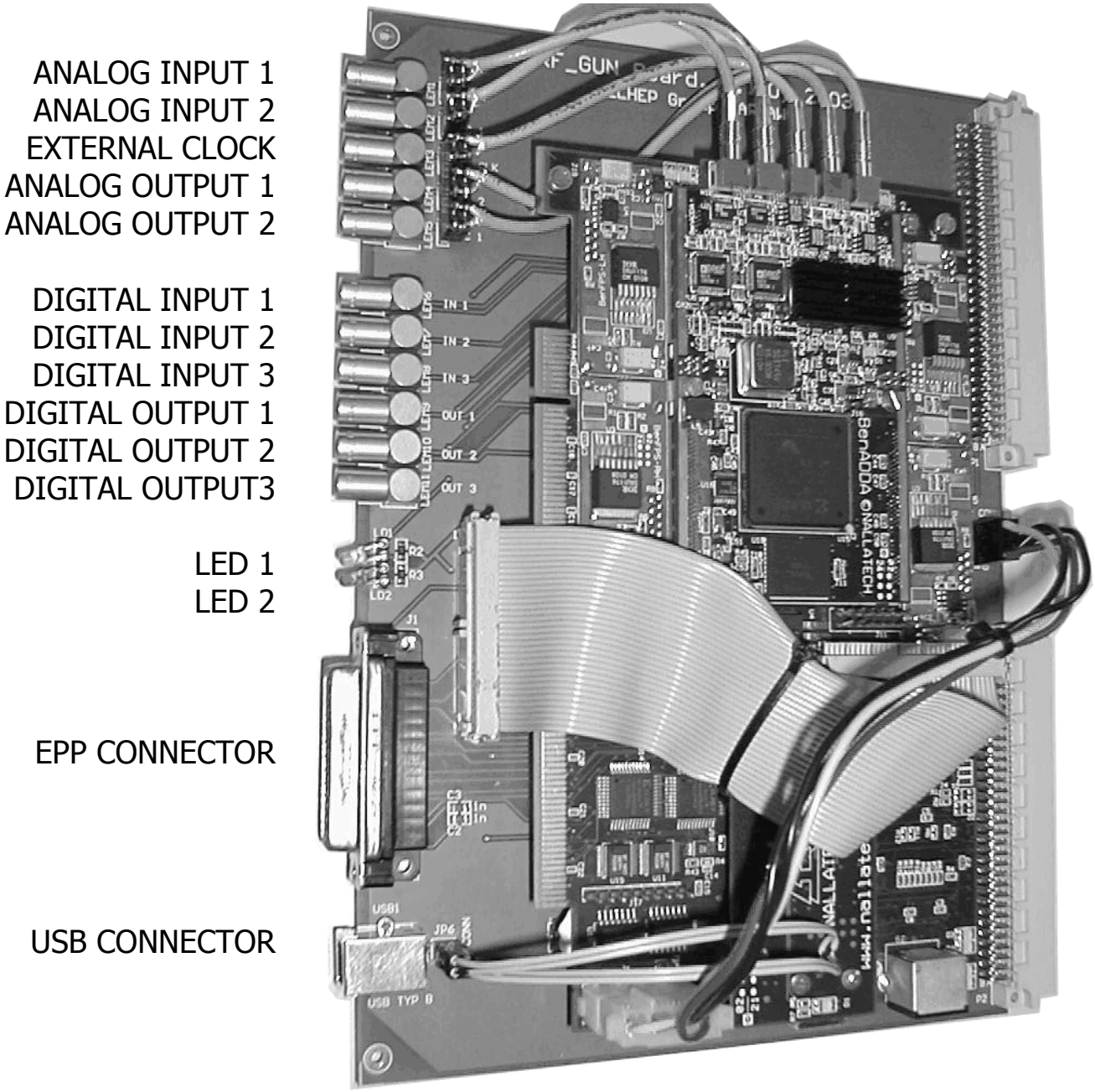

Figure 9. Hardware layer of the SIMCON system. PCI/USB kit board [4] positioned on the VME carrier

The integrated SIMCON system is realized in form of a parameterized structure of functional blocks in VHDL. The AD and DA converters are located on a daughter board. The optional connection of the external control to the simulator or controller of the FEL cavity is possible via the provided I/O ports. The digital TTL inputs, present on the VME board, were used for synchronization with the 1MHz clock and the 10 Hz trigger. A signal of 10Hz is the major trigger of the accelerator and 1MHz is the sampling frequency of the down-converted signal. These signals are distributed in the existing analog generation of the whole control system of the FEL. The functional structure of the SIMCON is presented in figure 10.

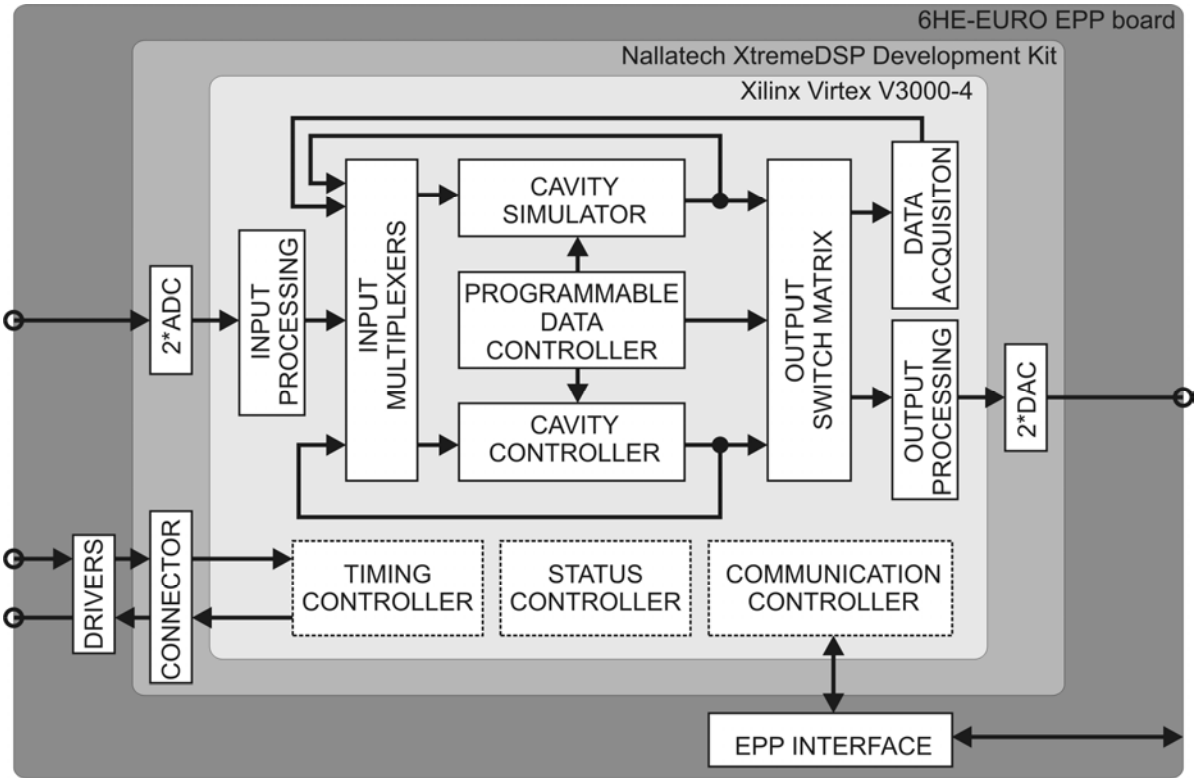

Figure 10. Multilayer functional structure of the SIMCON

A core of the SIMCON is built of two nondependent modules: the CAVITY SIMULTOR and the CAVITY CONTROLLER. They are programmed inside the FPGA chip as hardware DSP algorithms. The algorithms use fast internal multiplication components. The blocks work in parallel in real time. They are controlled by programmable parameters provided by the PROGRAMMABLE DATA CONTROLLER block. The parameters are scalars (cavity and controller data) and vectors (feed-forward and beam data). The set parameters stem from the algorithms described in detail in [3].

The block of INPUT MULTIPLEXERS allows the programmable input of the control signals of controller and simulator blocks. Realization of the following functions is possible through this block: internal digital feedback loops, connection of external analog signals from AD converters, setting of test vectors initially programmed in the DAQ block (described below). The OUTPUT SWITCH MATRIX selects different outputs to the DA converters or data registration in DAQ block. A suitable configuration of the switch matrix gives appropriate analog feedback between the cavity controller and simulator.

The block DATA ACQUISITION (DAQ) allows for current monitoring of the most important signals in the system. These may be input and output signals or internal results from the DSP processing in the algorithms of cavity simulator and controller. DAQ block is used as programmable signal generator for the tests of the input and output signals.

The block INPUT PROCESSING provides a conversion of values between physical 14-bit resolution of ADC converters and 18-bit resolution of internal DSP processing, the input signal calibration including amplification and regulated shift of the constant voltage value, as well as smoothing of the input channels (preprocessing) using a method of averaging. The block OUTPUT PROCESSING provides conversion between physical 18-bit resolution of the internal DSP processing and 14-bit resolution of DAC.

The block TIMING & STATUS CONTROLLER provides internal synchronization of all processes of the SIMCON system. It selects between the external clock signals provided by the accelerator control system or clocks from external generators. The latter case enables autonomous work of the system. Switching of the operation modes of the system is possible, i.e. performing simulation in real time or in the step simulation regime with reference vectors.

The programming layer of all blocks of SIMCON system is realized by the control computer system with the aid of the COMMUNICATION CONTROLLER block. The EPP hardware transmission protocol was used for this purpose. The signal distribution bases on the Internal Interface standard, described in detail in [7].

The step operation and vector stimulus mode is applied for testing the FPGA device coupled to the MatLab system via the COMMUNICATION CONTROLLER. The FPGA signal processing was verified according to the desired algorithm. To realize online processing, a synchronous 40MHz pipeline bus is used. The system flexibility, obtained in this way, gives the possibility to choose arbitrarily the number of clock periods necessary to do the successive, partial calculations by the DSP blocks.

5. Software simulation and results of hardware test procedure

The FPGA cavity simulator with controller is coupled to the Matlab system via a communication interface. The real time tests are carried out according to the schematic block diagram shown in figure 11. The Matlab system initiates the simulation process for given primary parameters of the cavity model according to table 1. The secondary, internal parameters for the FPGA system were calculated as described in the second paragraph. The required data for the Set Point and Feed Forward tables of the controller are generated according to the cavity model by an iterative processing striving to the optimal control. The Matlab simulation process is verified by a plot. The resulting example, for the real operational condition, is presented in figure 12. The cavity is driven in pulse mode forced by control feedback together with the direct control by feed-forward . During the first stage of the operation, the cavity is *filling* with a constant forward power, resulting in an exponential increase of an electromagnetic field, according to its natural behavior in resonance condition. When the cavity gradient reached the required final value, the beam loading current is injected, resulting in the steady-state *flattop* operation. Turning off both, the generator and the beam current, yields an exponential *decay* of the cavity field.

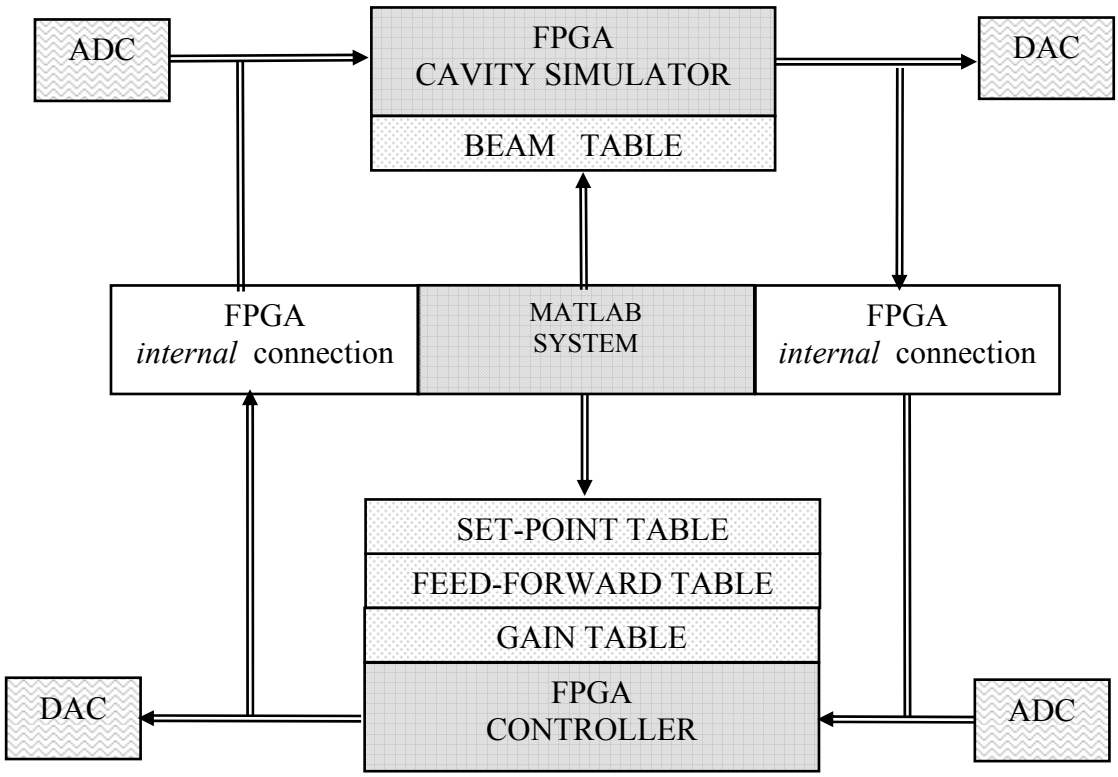

Figure 11. Functional diagram for the one chip FPGA system

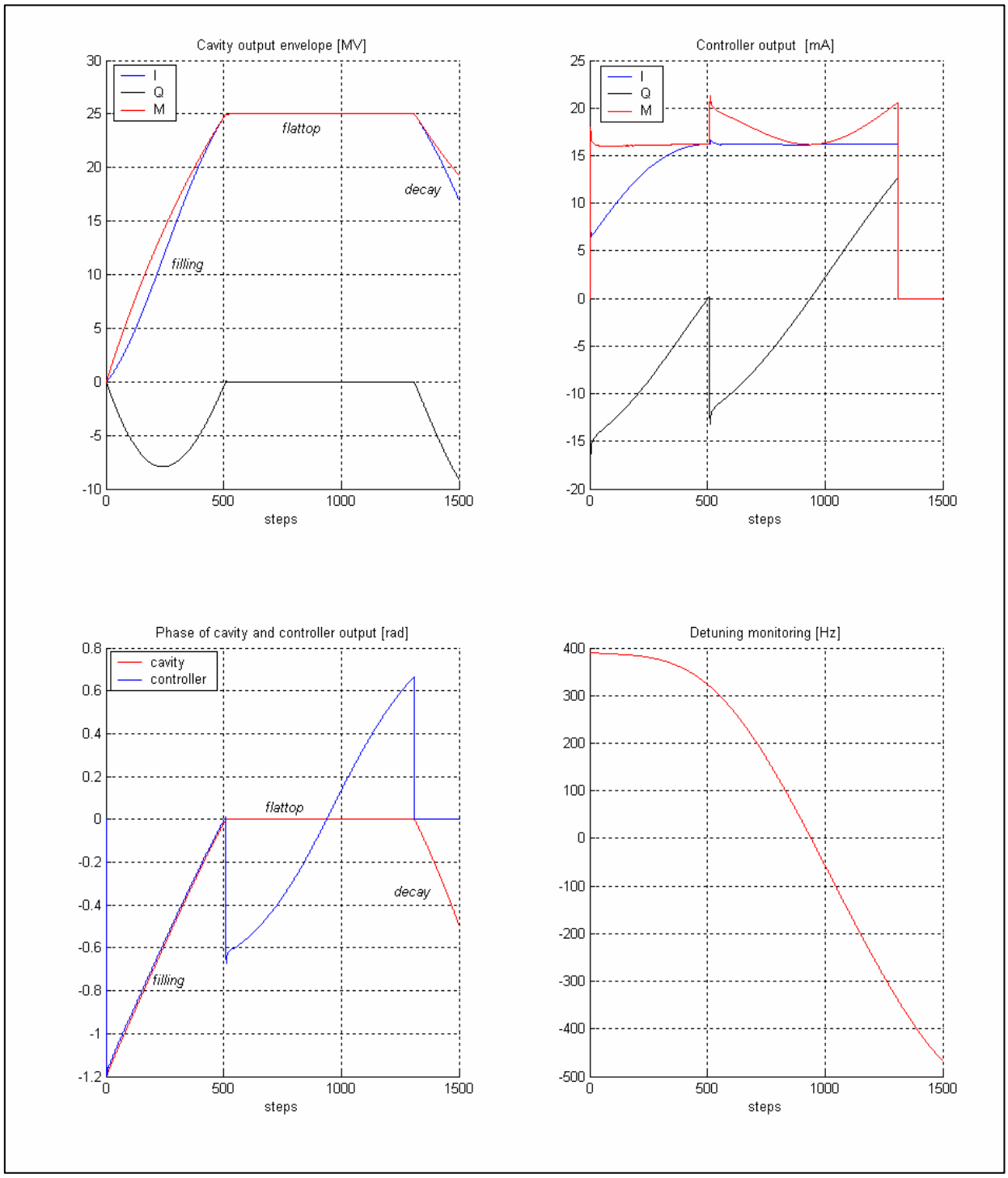

Figure 12. Matlab simulation of the cavity model for real operation conditions

The resulting parameters and data are loaded to the FPGA internal memory. The controller can drive the cavity simulator via the internal digital connection (18-bit data resolution). The FPGA system can run itself cyclically according to the given data tables. The cavity simulator and controller can be also driven independently via the external connection applying 14-bit ADC. The 14-bit DACs convey data from the cavity simulator or from controller outside FPGA system.

The real time tests were carried out according to the described simulation procedure. The FPGA system runs itself cyclically according to the given data tables and the output signals are monitored by oscilloscope. The simulation results corresponding to fig.12 are presented in figs. from 13 to 16.

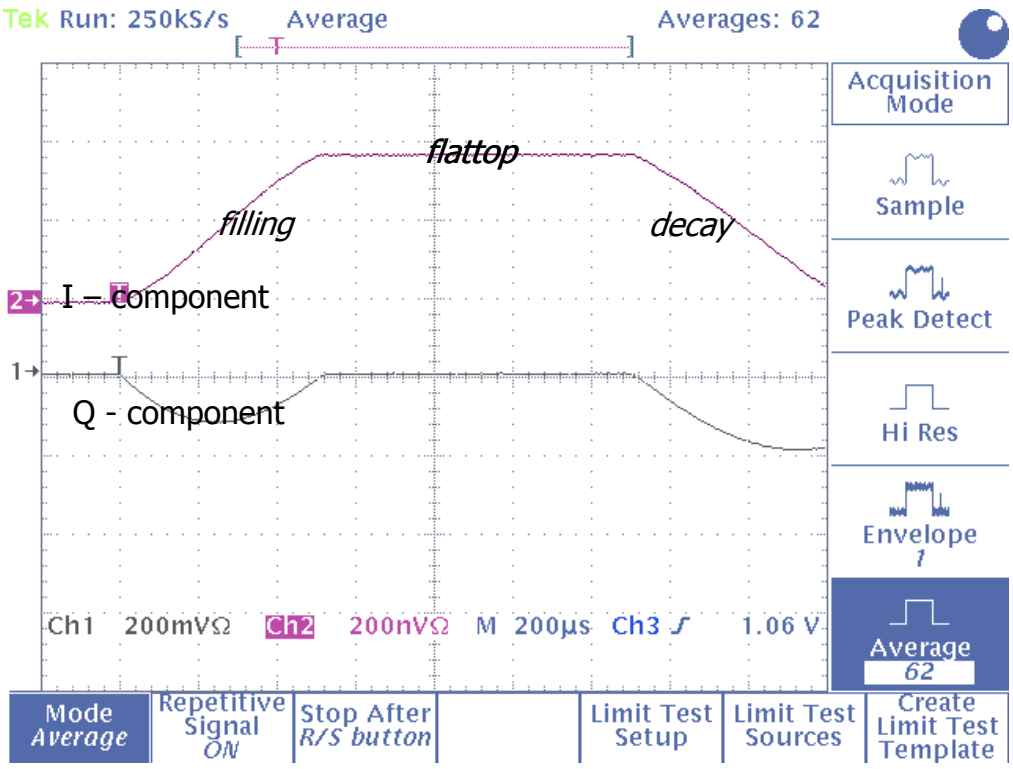

Figure 13. Output envelope of the cavity simulator driven by feedback and feed-forward mode

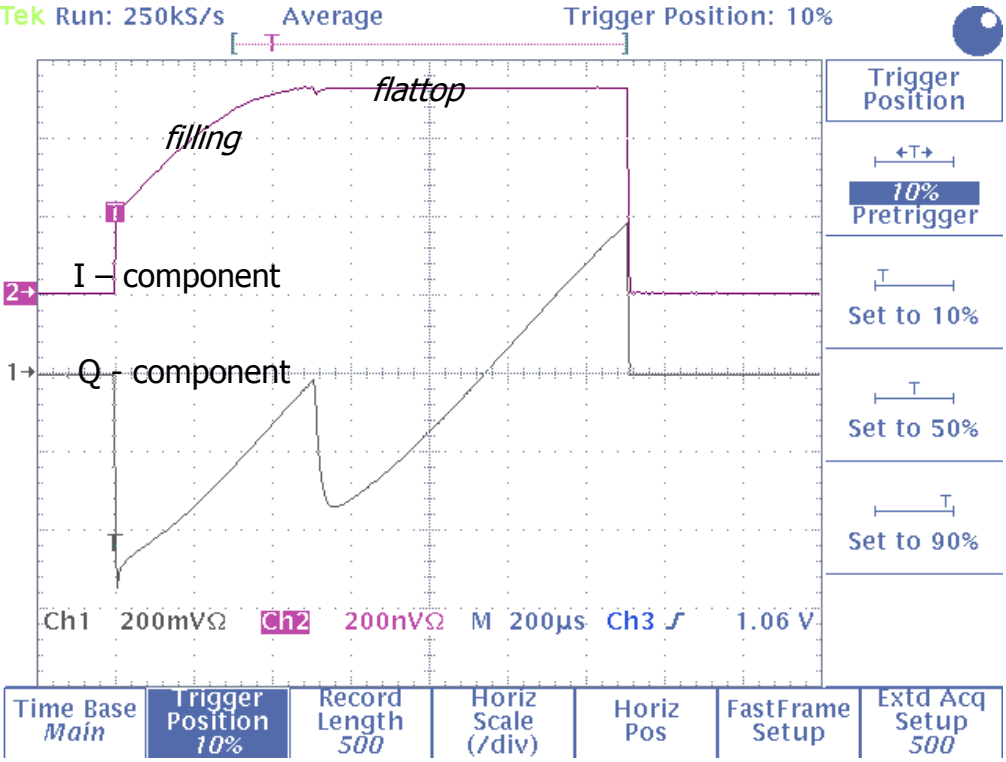

Figure 14. Output envelope of the cavity controller operated in feedback and feedforward mode

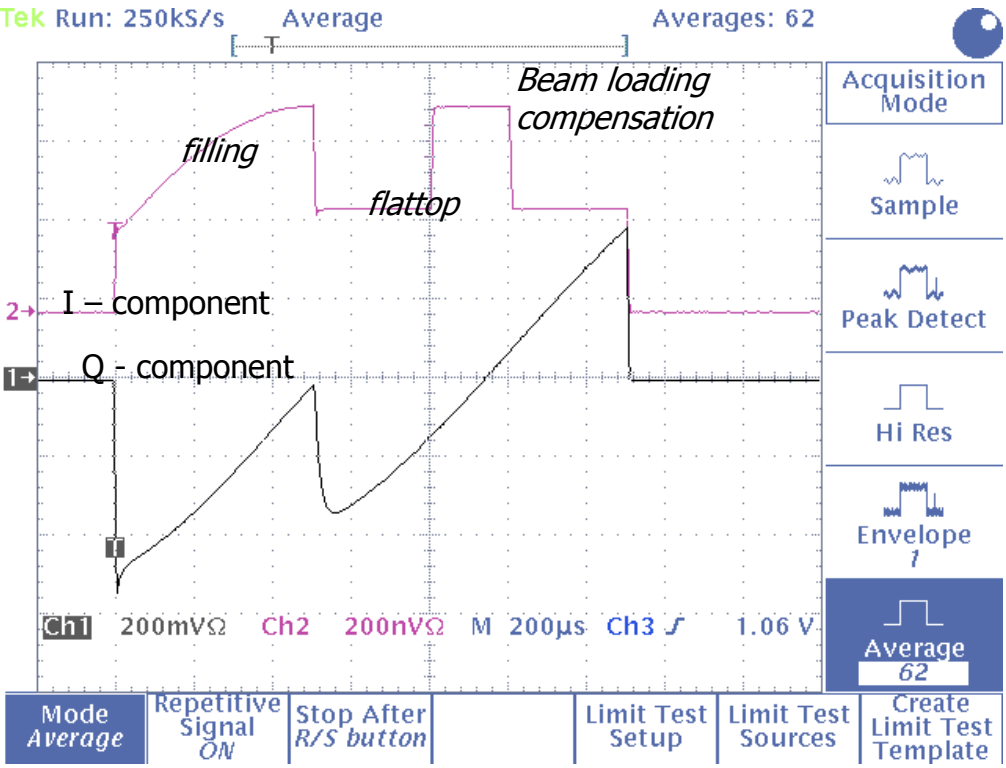

Figure 15. Output envelope of the cavity controller with short pulse beam compensation during flattop level

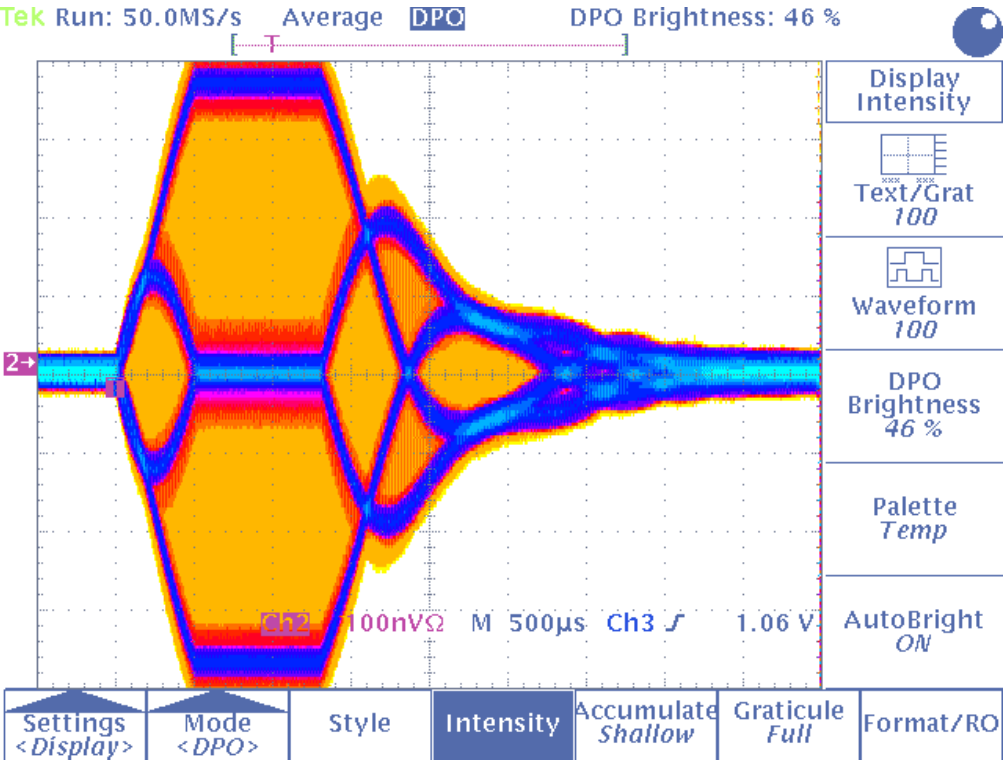

Figure 16. Cavity simulator output for the 250 kHz modulated signal

6. Conclusions

The TESLA cavity simulator integrated with controller has been implemented for the control system purpose, applying FPGA technology. An efficient DSP algorithm was developed describing a cavity model in a comprehensive way. Proper scaling of parameters and variables in the DSP program provides an optimal numerical precision for a given bit resolution. The FPGA cavity simulator has been investigated for different operational conditions: step response, feed-forward and feed-back mode. The step operation and vector stimulus method is proven to be efficient for testing a FPGA device coupled to the Matlab system. The FPGA implementation with 18-bit resolution is sufficient for simulation purpose and control system testing. The cavity simulator can be adopted for superconductive and normal conductive resonator models by applying different sets of parameters. The very confined resources occupied by the 18-bit resolution model (inside a single programmable chip) allow for prospective simulation and control of a large number of accelerator cavities by a single FPGA chip.

Acknowledgments

We acknowledge the support of the European Community Research Infrastructure Activity under the FP6 "Structuring the European Research Area" program (CARE, contract number RII3-CT-2003-506395).
The authors would like to thank DESY Directorate for providing excellent conditions to perform the work described in this paper.

References

1. T. Schilcher, “Vector Sum Control of Pulsed Accelerating Fields in Lorentz Force Detuned Superconducting Cavities”, Ph. D. thesis, Hamburg, 1998
2. M. Liepe, W.D.-Moeller, S.N. Simrock, “Dynamic Lorentz Force Compensation with a Fast Piezoelectric Tuner” in Proc. of the 2001 Particle Accelerator Conference, Chicago
3. T. Czarski, R.S. Romaniuk, K.T. Pozniak, S. Simrock, “Cavity Control System, Advanced Modeling and Simulation for TESLA Linear Accelerator”, TESLA Technical Note, 2003-06, DESY
4. http://www.nallatech.com/ [Nallatech Homepage]
5. K.T. Pozniak, T. Czarski, R. S.Romaniuk, “Functional Analysis of DSP Blocks in FPGA Chips for Application in TESLA LLRF System”, TESLA Technical Note, 2003-29, DESY
6. K.T. Pozniak, R.S. Romaniuk, K. Kierzkowski, “Parameterized Control Layer of FPGA Based Cavity Controller and Simulator for TESLA Test Facility”, TESLA Technical Note, 2003-30, DESY
7. K.T. Pozniak, M. Bartoszek M. Pietrusinski, “Internal Interface for RPC Muon Trigger electronics at CMS experiment”, Proceedings of SPIE, Photonics Applications II In Astronomy, Communications, Industry and High Energy Physics Experiments, Vol. 5484, 2004